Chapter 3

In ovo exposure of combination insecticide results in incomplete closure of ventral body wall of chick embryo

3.1. INTRODUCTION

The process of development begins with the fertilization where male and female gamete fuse to form a zygote. This single cell contains a full complement of the genetic material and undergoes a series of cell divisions and cell differentiation, to form a multicellular embryo. The embryogenesis encompasses four different stages of development namely the morula stage (an early embryo with 16 totipotent cells), the blastula stage (a hollow sphere of cells with blastocoel) the gastrula stage (defines the formation of three germ layers) and the neurula stage (marks the development of central nervous system). It is intriguing to know how these cells and tissues form organs that work in cooperative and orchestrated manner to form an organism. In contrast, any intrusion and distress arising from either genetic or environmental factors lead to the occurrence of developmental anomalies in the organism, putting its survival at stake. Patel and Adhia (2005) carried out a surveillance on birth defects showing 2.5 % infants with congenital abnormalities, out of which 15 % show mortality at perinatal stages. With this information in hand, we have noted that an acute exposure of a combination insecticide (Ci) caused a variable amount of birth defects in the developing chick embryo. The anomalies listed were distorted cephalization, umbilical hernia, ectopic viscera, spina bifida and anophthalmia (Uggini et al., 2012; Uggini and Suresh, 2013). Teratogenic potential of Ci was also reported to be passed onto the succeeding generation wherein only the parent generation received the dose of Ci (in ovo, preincubation exposure) as reported by Khan et al., (2015). There are a variety of etiological factors such as chromosomal aberrations, single gene defects, drugs and environmental toxicants causing birth anomalies in the humans and pesticides are one of them (Stevenson, 2015).

Pesticides have played an axial role in testifying the evolution of the chemical industry and its worldwide usage raises significant safety concerns in humans (Grube et al., 2011). Through the years they have stood the test of time as the front runners of chemical application by increasing agriculture yield. Such was the popularity of these pesticides that their capacity of bioaccumulation and biomagnification was hardly noticed until quite recently. Pesticides that accumulated extensively were majorly organophosphates and organochlorines, both which are banned today in most of the developed countries. It is well documented that the toxic manifestations of pesticides to humans occurs through food and water consumption, as well as through occupational exposure (van den Berg et al., 2012). Many of the pesticides are toxic to major systems of man and animal namely endocrine system, nervous system as well as immune system to name few in addition to being teratogenic (Blair et al., 2015). Moreover, a number of studies show that prenatal exposure and maternal proximity to agricultural fields sprayed with pesticides are associated with greater incidences of abdominal wall defects (Shaw et al., 2014).

3.2. VENTRAL BODY WALL CLOSURE DEFECTS

Abdominal wall defects are the most commonly occurring congenital malformations classified as ventral body wall defects (VBWDs). This group includes deformities such as ectopia cordis, gastroschisis, omphalocele, bladder exstrophy etc. Ectopia cordis (5.5-7.9/million live births) and bladder exstrophy (1/40,000 live births) are much rarer than gastroschisis (3.3/10,000) and omphalocele (2.5/10,000 live births) (Prefumo and Izzi, 2014). Majority of these defects do not have a genetic basis but are caused by a plethora of environmental insults. The defects in gastroschisis occur most likely due to abnormal closure of the body wall by the lateral body wall folds during the fourth week (post-fertilization) of development in humans. In contrast, omphalocele represents a separate entity where the bowel loops fail to return in the abdominal cavity and remain protruded throughout the development (Wilson and Johnson, 2004). Most teratogenic effects today trace their etiology down to the chemical residue (pesticides in this case) present in the environment around the developing embryo. During development, lateral body folds play a major role in closing the ventral body wall. There are various hypotheses explaining how the ventral body wall defects arise and one of those theories which gained support was proposed by Duhamel (1963). The theory attributes this to teratogenic insult to the lateral body folds or during the process of organogenesis, which results in celosomia (hernia of abdominal wall). These folds arise from the parietal layer of lateral plate mesoderm and continue to move ventrally towards the midline where they fuse (Feldkamp et al., 2007). Unfortunately, this theory has been largely overlooked. However, it is probably the best explanation for how the defect arises and has recently gained additional support (Sadler, 2010).

3.3. FORMATION OF VENTRAL BODY WALL

In order to gain insight on the occurrence of ventral body wall closure defects, it is mandatory to explicate the mechanisms of body wall closure and the role. Also, it is obligatory to understand the contribution of lateral folds in bringing the ventral wall closure. In the later part of the gestation period, the embryo is in the shape of an elliptical disk. This disk has three germ layers in the cranial portion namely the ectoderm, dorsally mesoderm and ventrally the endoderm (Sadler and Feldkamp, 2008). Along with the neural tube development changes occur in the mesoderm layer indicating the formation of the body folds and body cavity. This germinal layer further compartmentalizes into three different regions:

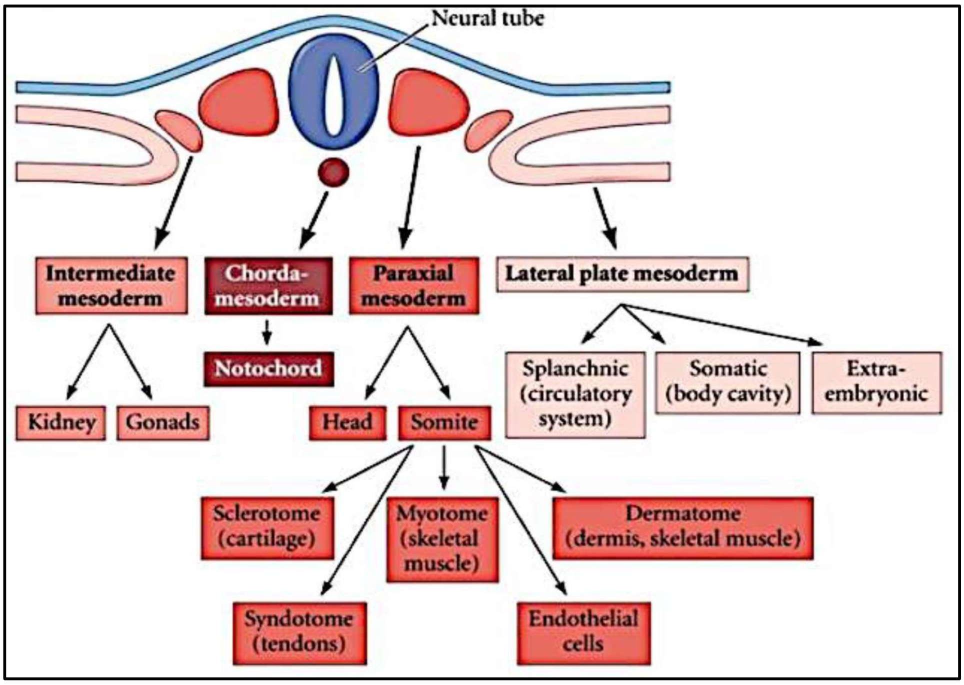

Figure 3.1: Schematic representation of mesodermal lineage in Amniotes. Source: Bess and Varma, 2011

1) **Paraxial mesoderm**, that is present sideways to the neural tube. It arranges itself into a whorl of cells called somitomeres that further epithelialize to develop into somites. These blocks ultimately contribute in the formation of the skull, vertebrae, ribs, skeletal muscle, and dermis for skin covering the back.
2) **Intermediate mesoderm**, lying lateral to paraxial mesoderm which subsequently contributes to development of urinogenital system and;
3) **Lateral plate mesoderm** rips apart to bring the body cavity in existence. It further gives rise to membranes to cover the vital organs such as heart and lungs. Other derivatives are the limb bones, coastal cartilages and cavity associated with these structures (Hamilton and Mossman, 1972; Sadler and Feldkamp, 2008; Sadler, 2010) (Figure 3.1; 3.2).

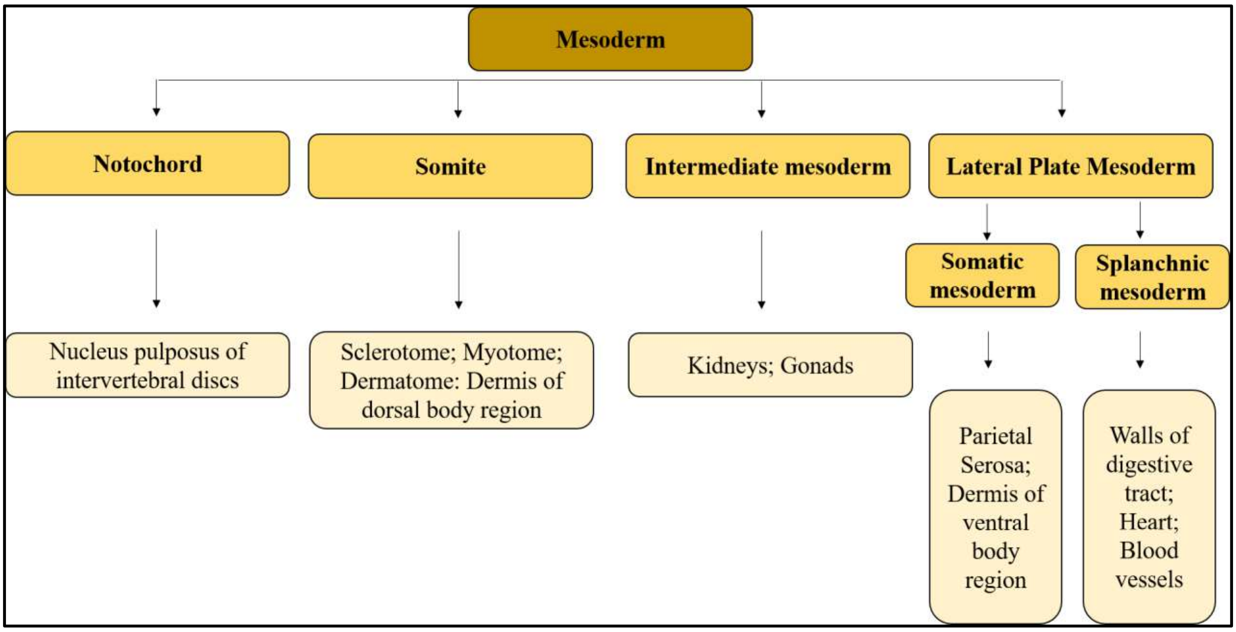

Figure 3.2: Image depicting various derivatives of mesodermal origin. Adapted from: **Gilbert, 2003**

Further, this lateral plate mesoderm forms a solid block of tissue continuous with extraembryonic mesoderm covering the amnion and yolk sac. Meanwhile in the development, small cavities appear that in this layer which merge to form two new layers surrounding a new cavity. The cavity then eventually gets parted into the pericardial, pleural and peritoneal cavities. This new mesodermal layer has parietal/somatic (present on the inner lining of the body wall) and visceral/splanchnic layers (lining the inside of the cavity). The parietal layer is strictly allied with ectodermal layer covering the body wall, whereas the visceral layer is closely associated with the wall of the gut tube (Christison-Lagay et al., 2011) (Figure 3.3).

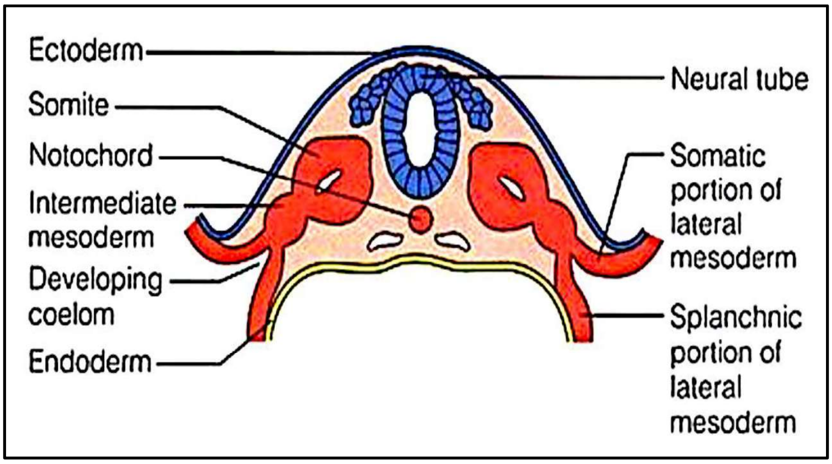

Figure 3.3: Embryonic development showing different mesodermal derivatives extending towards ventral side of the body. Adapted from: Gilbert 2003

The neural tube and ventral body wall closure occur simultaneously. The neural tube progresses towards the dorsal side of the embryo for closure whereas the parietal layer of the mesoderm along with the ectodermal layer moves towards the ventral side to cover the sides of the embryo. These structures form the lateral body folds that commence their downward extension to conceal the embryo ventrally. Both the cranial and caudal folds once formed, begin to fold the embryo that later develops in the foetal position. The combined movement of all the aforementioned body folds especially the visceral layer of lateral plate mesoderm and underlying endoderm merge in the midline and assist in formation of the gut tube. The tube extends from the pharynx to the anal canal and for most of its length it is suspended from the dorsal body wall by a dorsal mesentery derived from lateral plate mesoderm at the junction of the visceral and parietal layers (Prefumo and Izzi, 2014) (Figure 3.4).

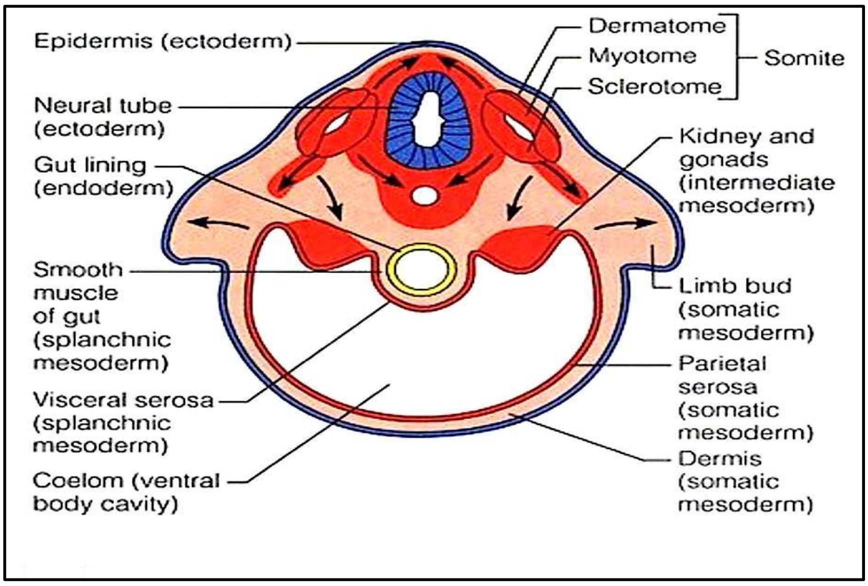

Figure 3.4: Mesodermal derivatives in the embryo showing progressive development to bring the ventral body wall closure. Adapted from: Gilbert 2003

3.4. DERIVATIVES OF SOMITES

In addition to these body folds, other potential contributors or forces that help in the movement the lateral body folds ventrally may be derived from somites. These paired segmental blocks are formed in the paraxial mesoderm towards the dorsal side and also differentiate into various components. Mesodermal cells transform to epithelial cells and get organized around the lumen after which they undergo epithelial to mesenchymal transition as they differentiate into bone, muscle, and dermal precursor derived from their sclerotome, myotome and dermatome regions respectively (Sadler and Feldkamp, 2008; Sadler, 2010).

Based on the above stated processes, it is easy to envision the defects in the closure of ventral body wall folds that lead to ectopia cordis, gastroschisis, bladder and cloacal exstrophy, Cantrell pentalogy and other related abnormalities. Each one of these can most likely be related to the failure of one or both of the lateral body wall folds to move far enough ventrally to meet its counterpart in the midline (Duhamel, 1963). Apart from this, secondary abnormalities can also occur through these defective regions such as diaphragmatic hernia and omphalocele observed in Cantrell pentalogy (Sadler and Feldkamp, 2008).

3.5. THE EARLY GENE EXPRESSION

The fusion of the body wall folds on the ventral side possibly involves important cellular processes like programmed cell death (apoptosis), formation of specialized cell-to-cell contacts and cell migration (Copp et al., 2000; Colas and Schoenwolf, 2001). A coordinated and timely activation and deactivation of each of these processes efficiently leads to the closure of body wall. These cell processes are governed by various important molecules such as SHH (sonic hedgehog), WNT, BMP (bone morphogenetic protein) and PITX2. SHH, one of the early expressed pattern forming genes plays a significant role in most of the above discussed cellular processes. It's synchronised activity with BMP, regulates the patterning of the somites in developing embryos. Moreover, inhibition of BMP4 by SHH controls its temporo-spatial expression, thereby holding the LPM from extending medially and ventrally (Marcelle et al., 1997; Gilbert, 2003). The BMPs are known to have a dual role in organising the event of body wall closure wherein, expression of BMP4 in dorsal neural tube, promotes muscle differentiation, its ectopic expression in the paraxial mesoderm, inhibits myotome formation. Moreover, the movements of mesodermal layers are under the control of cell adhesion molecules *viz.* CDH1. A coordinated expression of these genes orchestrates the closure of the body wall and hence, it would be interesting to study the effects of pesticides on the expression status of these regulators and their downstream effector molecules. It would be intriguing to investigate how the altered expression patterns of these genes and the alternative repair mechanisms, if any, which are activated to continue development even in the face of such an adverse chemical infiltration.

3.6. OBJECTIVE OF THE STUDY

Experimental studies carried out in mice and chicken have relied on gene knockouts, surgery, irradiation and exposure to environmental chemicals to produce VBW defects (Sitarek, 2001; Thompson and Bannigan, 2001; Singh, 2003; Williams, 2008). Among the environmental factors, the pesticide exposure has growing concerns over their potency of inflicting teratogenic effects. However, the precise molecular signalling by which the combination insecticide disrupts the early embryogenesis and causes VBWD is still stays unknown. The events of embryonic development like cell migration, proliferation and production of extracellular matrix are all vital for the completion of organogenesis and therefore, for the closure of ventral abdominal body wall too. Here we hypothesized that Ci interrupts the expression patterns of certain early molecular signals which take up the function of embryonic events like cell proliferation, survival as well as patterning and hence, might have led to the ventral body wall defects. In order to test this hypothesis, a mechanistic study on combination insecticide (Anaconda 505) induced VBWD was envisaged using chick embryo as model.

3.7. MATERIALS AND METHODS

3.7.1. Test substance

A commercially available insecticide formulation retailed as Anaconda 505^{TM} was used for the study. It constituted a combination of chlorpyrifos (50%) and cypermethrin (5%) and manufactured by AIMCO Pesticides Limited, Mumbai, India.

3.7.2. Egg procurement and insecticide injections

Freshly laid fertile eggs of Rhode Island Red breed of domestic chicken were obtained from the Intensive Poultry Development Unit, Vadodara, India. Eggs were cleaned, for external contamination if any, with 0.5 % povidone iodine solution and were kept at 4 °C until use. The concentration of sub-lethal dose was decided from the previous work done in the lab (Uggini et al., 2012). The eggs were dosed by air sac method as devised by Blankenship et al., 2003, on day "0" of incubation. The control group received olive oil (Figaro, India) and the treatment group was administered with 0.05 µg per egg of Ci with olive oil as vehicle, in a sterile environment in laminar air hood. The injection volume was kept 50 µl/egg. After dosing, the point of injection on the eggs was sealed by molten paraffin wax.

3.7.3. Incubation

Automated incubator (Scientific Equipment Works, New Delhi) was set at a temperature of 37.5 °C ± 0.5 and relative humidity of 70-75 % for incubation. The eggs were kept with their broad ends facing upwards and were turned automatically every 1 hour. The eggs were candled every two days and the dead ones were scrapped out. The experimental protocols were in full compliance with the guidelines of Drugs and Cosmetics rules 1945, Appendix-III animal care standard and were approved by the institutional animal ethics committee constituted as per the laid norms of the Indian regulatory authority (Protocol No. IAEC 84/08/2014-2).

3.7.4. Rate of mortality and malformations

After incubation, the embryos that had reached Hamilton-Hamburger stages 13 (day 2), 24 (day 4) and 36 (day 10) were collected. The somites were observed in day 2 embryos while rate of mortality and malformations were recorded in the day 4 and day 10 embryos. The experiment was performed thrice with 30 eggs in each time.

3.7.5. Histological studies

Embryos were isolated, rinsed in PBS and then were fixed in 10 % neutral buffer formalin. The tissue was further processed, and paraffin wax blocks of the tissue samples were prepared. Longitudinal sections (5 µm) of day 4 embryos and cross sections of 5 µm thickness of day 10 embryos were taken and stained with Harri's haematoxylin and eosin. The histological details of the tissues on the slide were visualized using Leica DM2500 microscope and pictures were captured using EC3 Camera (utilizing LAS EZ software).

3.7.6. RNA isolation and Real Time Reverse Transcription Polymerase Chain Reaction

The chick embryos were quickly dissected to excise the abdominal tissue. From this sample, total RNA was isolated by TRIzol reagent (Applied Biosystems, USA) as per the recommended protocol. 1 µg of total RNA was reverse transcribed to cDNA using a one-step cDNA synthesis kit (Applied Biosystems, USA) as per manufacturer's protocol. The genes considered for the present study were *SHH, PITX2, CDH1, BMP4, CASPASE 3, VIMENTIN, FGF8, CDH2, BMP1, PCNA, WNT11, WNT6, PAXILLIN (PXN), MYOD1, AHR, CYP1A1, CYP3A4, CYP3A5* and *18S rRNA*. The primer sequences of these genes are given in materials and methods section. Quantitative real-time PCR was performed using LightCycler 96 (Roche Diagnostics, Switzerland). After initial denaturation step of 3 min at 95 °C, 42 cycles of amplification for each primer was carried out. Each cycle included a denaturation step for 10 s at 95 °C, an annealing step for 10 s at 60 °C and elongation for 10 s at 72 °C. Melt curve analysis was used to confirm specific product formation. Data was represented as mean Cq values normalized with 18S rRNA (endogenous control) levels and fold change in expression was calculated using the $2^{-\Delta\Delta Cq}$ method of Livak and Schmittgen (2001).

3.7.7 Western blot

Tissue from the abdomen region was collected from four embryos of each experimental group and homogenized in Tris-SDS lysis buffer with protease inhibitor (Sigma Aldrich, USA). 10 % homogenates were assayed for total protein content by Bradford method (1976) Equal amount of total protein was loaded and separated by SDS-PAGE on 12 % gels. Protein was transferred onto PVDF by semi-dry transfer at 100mA for 20min. The membrane was probed separately with anti-SHH, anti-β-Actin (IgG antibodies raised in Mouse) and anti-CASPASE 3 (IgG antibodies raised in Rabbit). Alkaline phosphatase system was used for staining the protein of interest.

Further, Spot densitometry was performed on all the bands using Doc-ItLS software (GeNei Imaging systems, India). The densitometric values were used to compare the bands of interest and the results were expressed in arbitrary units.

3.7.8. Statistical analysis

Abnormalities in somite number were subjected to Mann-Whitney U Test to compare differences between the groups. The rest of the data was analysed by two-tailed Student's t-test using Prism v5.03 (GraphPad Software Inc., USA). Values were expressed as Mean ± SEM, and the differences between the control and treated groups were considered significant when the P value was less than or equal to 0.05.

3.8. RESULTS

3.8.1. Rate of Mortality and Malformation

The pesticide dosed embryos were opened for examination on day 2 (stage 13), day 4 (stage 24) and day 10 (stage 36). The stage-13 control embryos showed the standard features i.e. presence of twenty somites, broad curves in cranial and cervical flexures and well-established stalk. The embryos treated with 0.05 µg of Ci after incubation of 2 days showed significantly reduced number of somites. Moreover, 33 % of the embryos showed abnormal somite disposition (Table 3.1). High rate of mortality and anomalies were observed in all the treatment groups. A steep rise ($p \leq 0.001$) was observed in the mortality of embryos in pesticide dosed groups as compared to the control and it continued to increase as the embryo developed to day 10 (Table 3.2). As the study was focused on ventral body wall defects, the rate of occurrence of these malformations was checked. It was observed that in the treatment group 60.6 % of the total live embryos observed on day 10 had defects in their abdominal wall closure, whereas the embryos from the control group showed no overt signs of abnormalities (Table 3.3).

3.8.2. Teratological malformations

When the embryos were examined at stage 24, the controls showed normal development with distinct eye pigmentation and limb buds (Figure 3.5A). However, defects like microphthalmia, and stunted growth were found in day 4 incubated treated embryos (Figure 3.5B). While the control embryos (Figure 3.6A) examined on day 10 showed normal patterns of development of visceral organs and the abdominal wall, the treated embryos showed protrusion of heart, bowel and liver due to defect in midline fusion of abdominal wall (Figure 3.6B). The other associated anomalies included anophthalmia, phocomelia, hematomas, stunted growth and defect in ventral body wall closure in the thoracic region (Figure 3.7 A, B, C, D).

3.8.3. Histopathology

The extent of damage caused by the pesticide load in the tissue architecture was studied by differential staining in day 4 and day 10 chick embryos by using haematoxylin and eosin. The control embryos on day 4 showed properly arranged somites with well-developed myelencephalon and optic cup (Figure 3.8A; 3.9A). The heart was well formed with clear demarcation between atrium and the ventricle. The treated embryo showed stunted growth, with a reduction in the somite numbers and distorted optic cup (Figure 3.8B; 3.9B). The histological picture of day 10 embryos exposed to Ci showed less developed musculature and the internal organs were left uncovered. A striking feature observed in the treated embryo was absence of sternum (Figure 3.10 B, 3.12) when compared to control embryos (Figure 3.10 A, 3.11).

3.8.4. Relative mRNA expression levels

In day 4 embryos, the relative mRNA expression levels of *SHH* were found to be significantly lowered ($p \leq 0.001$) in the treatment groups when compared to the controls, the *BMP4* ($p \leq 0.001$), *PITX2* ($p \leq 0.05$), *CDH1* ($p \leq 0.001$) and *CASPASE 3* ($p \leq 0.001$) were found to be significantly increased in the treated group. However, no significant changes were seen in case of *CDH2* and *FGF8* expression (Figure 3.13; Table 3.4).

The qRT-PCR analysis in day 10 embryos showed that along with *SHH*, the *CDH1*, *WNT11* and *WNT6* expressions were significantly upregulated ($p \leq 0.001$). Nonetheless, the change in expression levels of *VIMENTIN* was found statistically insignificant. However, *PXN* ($p \leq 0.05$)

expression was found to be increased. While the mRNA levels of *BMP1* remained unchanged, the levels of *MYOD1* have significantly gone high ($p \leq 0.01$) in the treated embryos. The *PCNA* and *CASPASE 3* showed a highly significant ($p \leq 0.001$) decrease and increase respectively. *AHR* ($p \leq 0.001$) and *CYP3A4* ($p \leq 0.05$) expression increased with significance, while *CYP1A1* ($p \leq 0.05$) and *CYP3A5* ($p \leq 0.01$) showed a downregulation (Figure 3.14; Table 3.5).

3.8.5. Western blot analysis

In order to reaffirm the results of transcript level analysis few representative proteins from various pathways or processes highlighted earlier were quantified through western blot. Immunoblot analysis revealed reduced expression of SHH in the treated embryos on day 4 compared to that of in the control. This confirms that sonic hedgehog levels were reduced at both transcription and translation levels by pesticide intoxication. On day 10, E-Cadherin and CASPASE 3 levels were found to be increased and hence, validated the qRT-PCR results (Figure 3.15; Table 3.6). β-actin was used as internal control.

3.9. DISCUSSION

Having known that toxicants like Ci are capable of inducing teratological manifestations in the developing embryos, the current study was designed to look for the underlying changes in the molecular mechanisms. The visual and microscopic observations of the treated embryos on days 2, 4 and 10 showed several teratological and histomorphological aberrations, amongst which the ventral body wall defects have been chosen for an elaborate study. The treated embryos which showed the VBWD had an exposed viscera protruding out of ventral abdominal wall due to a failed midline closure.

The VBW formation can be traced back to its embryonic origin from the mesoderm formed during the gastrulation. Several studies were conducted in the past on different embryonic models, to understand the formation of the ventral body wall. The contribution of lateral plate mesoderm and paraxial or somatic mesoderm towards the formation of ventral body wall was discussed earlier by Sadler and Feldkamp (2008). The etiologies of failure in the formation of VBW were also investigated. These studies discussed about the embryonic dysplasia, vascular disruption, mechanical disruption, and also a disruption in the crosstalk between the epithelium and mesenchyme of the gastrulating embryos as the possible candidates leading to defects in VBW. The role of various pattern forming genes like WNT, PITX2, BMPs, and cell adhesion molecules too were elaborated (Kitamura et al., 1999; Brewer and Williams, 2004; Sadler and Feldkamp, 2008; Matsumaru et al., 2011; Snowball et al., 2015).

However, SHH, one of the early expressed pattern forming genes plays a significant role in most of the above discussed cellular processes. SHH and its synchronised activity with BMP4, regulates the patterning of the somites in developing embryos. Also, SHH controls the temporo-spatial expression of BMP4 signal by inhibiting it, and holding the LPM, from extending medially and ventrally (Gilbert, 2003). The BMP is known to have a dual role, while expression of BMP4 in dorsal neural tube promotes muscle differentiation, its ectopic expression in the paraxial mesoderm results in inhibition of myotome formation. Consequently, a proper myotomal development would also require the BMP to be inhibited at the paraxial mesoderm in a specific temporal manner (Marcelle et al., 1997). In the present study, the mRNA expression analysis on day 4 showed that the Ci treated embryos had a downregulation of *SHH* and upregulation of *BMP4* when compared to the control embryos. This dysregulation in the expression of *SHH* and *BMP4* must have created the initial disturbances in the paraxial mesoderm, thereby disrupting the somite patterning and subsequently must have caused anomalies in the myotome differentiation too in the embryos.

Further, under normal conditions there is a differential expression of *PITX2* on the embryonic left and right sides resulting the axis formation, which is controlled upstream by selective inhibition of *BMP4* and *FGF8*. Though the changes in *FGF8* expression remained insignificant, the increased expression of *BMP4* and *PITX2* in the exposed embryo indicates a disparity. Contrary to our observations with regard to PITX2, according to Kitamura et al., (1999) deficiency of PITX2 caused a failure of ventral body wall closure in mice, and they have also observed that the PITX2 deficiency was influenced by a different genetic cascade other than FGF8 derived. In another study by Fung et al., (2012) upregulated PITX2 is indicated during oncogenic progression, where PITX2 might be contributing towards the growth and migration of cells. Also, there are reports indicating that an elevated PITX2 ropes in the free radical scavenging by promoting the gene expression of antioxidants (Tao et al., 2016). Therefore, an increased expression of *PITX2* here might be an embryonic response to induce the formation of antioxidants against the stress induced by the Ci exposure. In addition, it has been documented that during the metabolism of pyrethroids, free radicals are liberated via oxidative pathways by cytochrome P450 microsomal enzyme system that damage the liver and cause an increase in the levels of serum enzymes in chicken hatchings (Uggini et al., 2012). To further understand this response, we tried to look into some of the indicators of xenobiotic metabolizing mechanisms. The aryl hydrocarbon receptor (AHR), which is a ligand associated transcription factor acts like a xenosensor and has a role in upregulation of the cytochromes which subsequently work on metabolizing the xenobiotics (Stevens et al., 2009). In the current study, we observed a very significantly upregulated *AHR* and *CYP3A4* expressions in day 10 embryos, which is a clear indication of combat to overcome the stress laid by the Ci. However, an overburden of the extraneous agent when not efficiently dealt by the clearance pathways might culminate into dire consequences like renewal of teratogen targeted cell population by inducing apoptosis (Torchinsky, 2005). Our study shows a highly significant increase in the expression of *CASPASE 3* activity in both day 4 and day 10 embryos which can be correlated to the large-scale apoptosis occurring in the Ci treated embryos. At the same time the levels of *PCNA* were found to be downregulated indicating that the cell proliferation was hampered. Moreover, activation in the SHH signalling pathways is seen under conditions of oxidative stress and could regulate cell proliferation and apoptosis (Heine and Rowitch, 2009; Xia et al., 2012). In concordance, we have observed an upregulated expression of the *SHH* in the day 10 Ci treated embryos relative to the controls.

Furthermore, the somitogenesis, LPM formation and movement of lateral body folds are governed by cellular activities like programmed cell death, intercellular crosstalk, cell migration and cell proliferation (Copp et al., 2000; Colas and Schoenwolf, 2001). In the developing embryos, the migrating cell is highly polarized and is regulated by complex set of signals. The differentiating new cell types depend upon a finely balanced and coordinated regulation of gene expression and precise interaction amongst their neighbours. We, therefore, also sought to identify few such molecular signals that regulate the said processes. The expression of *CDH1*s during embryonic development happens quite early where they play a role in adhesion and compaction of the blastomeres. It also signals the controlled epithelial-to-mesenchymal conversion and regulates developmental processes like cell migration and proliferation (Fleming et al., 1992; Barth et al., 1997; Kalluri and Weinberg 2009; Bahm et al., 2017). The migration of mesodermal cell is favoured by downregulation of the CDH1 and loss of cell adhesion (Ciruna and Rossant, 2001; Basson, 2012). Our results have shown that levels of *CDH1* were found to be upregulated in both the day 4 as well as day 10 Ci treated embryos, giving clear evidence that the cell migration was delayed and/or hampered. Further, the *CDH1* is known to be downstream target of *SHH* (Xiao et al., 2010), which means that an inhibition of *SHH* would result in decreased *CDH1* expression. However, our results contrastingly have shown that the SHH was downregulated while CDH1 was upregulated in the 4 day treated embryos, while in day 10 treated embryos, both were found to be upregulated. This indicates that *CDH1* though regulated by *SHH*, might as well be under the control of some other upstream signal. A negative correlation between the SHH and CDH1, nevertheless, was reported during metastasis (Karhadkar et al., 2004; Sun et al., 2017). Further, the PXN, which is a multifunctional focal adhesion adaptor protein, was found to be upregulated here. PXN expression has its significance not only during embryonic development and cell movement, but also elevated levels of PXN are found in pathological conditions like oxidative stress and metastatic cancers (López-Colomé et al., 2017). An elevated *PXN* observed in day 10 treated embryos could as well be related to the condition of oxidative stress caused by the Ci exposure. Earlier studies by Ray et al., (2010) in neonatal rats has also shown that chlorpyrifos administration leads to differential expression of genes like PXN involved in cell adhesion and migration.

Subsequently studies were extended to understand the pattern of WNT expression. The WNT signalling plays a significant role in abdominal myogenesis and formation of secondary ventral body wall. Additionally, WNT11, a non-canonical WNT member, has a role in cell adhesion and movement. The WNT11 and WNT6 are cited to be pivotal in maintaining the epithelial nature of the dorso-medial and ventro-lateral lips of dermomyotome and a deficit would lead to defects in the ventral musculature formation (Zhang et al., 2014). However, our study has shown a significant upregulation of *WNT11* and *WNT6* in the Ci treated embryos on day 10. Nevertheless, such aberrant upregulation of the WNT signalling pathways has been reported after a chronic exposure to cadmium in mouse (Chakraborty et al., 2010) and also in many cases of malignant human cancers (Loh et al., 2013).

Furthermore, a review by Wang et al., (2004) bring into fore the role of *BMP4* in early developmental process, where, an absence of it leads to failure of mesoderm formation. However, at a later stage, *BMP1* deficiency would lead to the defects in ventral body wall closure. In addition, it is well documented that MYOD expression is a marker to the early myoblasts (Zhang et al., 2014). A relatively higher expression of the *MYOD1* in the treated embryos could be an indication that the myoblasts remained so and failed to undergo further differentiation in the intoxicated embryos. Visual clues to this failure of muscle differentiation could be drawn from the histological sections of the embryos. Further, it has been reported that sonic hedgehog regulates MYOD expression to enhance the embryonic skeletal myogenesis (Voronova et al., 2013). Here an upregulation of *MYOD1* would have been subsequent result of

SHH upregulation, discussed earlier. Thus, the signalling molecules discussed above provide possible clues about mechanism of Ci toxicity and their aberrant signalling led to defects in ventral body wall.

3.10. CONCLUSION

Visual and microscopic observations and the mRNA profiling of the molecular signals regulating the processes like epithelial-to-mesenchymal transition, cell proliferation, migration and survival or death were sought for, in the Ci treated chick embryos. We observed that the fate of these embryonic cells, which constantly rely on interpretation of the signals from their neighbours and surroundings, show a larger erroneous display in not just a single pathway, but in the intricate regulatory networks. The alterations came up in a way more complicated than do a single gene knockout studies that lead to the ventral body wall defects. There was an initial drop in the *SHH* in day 4 embryo and elevation in day 10, however the other observed morphogens namely the *BMP4, WNT11, WNT6*, and markers for cell differentiation, EMT, apoptosis and oxidative stress like the *PITX2, CDH1, PXN, MYOD1, CASPASE 3, AHR, CYP3A4*, were upregulated on day 4 as well as on day 10 of embryonic development, showing similarity to the state of oxidative burden and also malignant cancers. The developing embryonic mechanisms while metabolizing the toxin and clearing the oxidative burden, might face a grave consequence due to changes in signal strength and might have ultimately lost their potency to achieve the developmental milestones, the completion of ventral body wall formation being amongst them.

3.11. SUMMARY

There are evidences that connect the casual relationship of rampant usage of insecticides and the development of structural malformations in the non-targeted species. Our previous studies revealed that, in chick embryos, a preincubation exposure to a commercially available combination insecticide (Ci, 50 % chlorpyrifos and 5 % cypermethrin) lead to the formation of several teratological malformations, amongst which, ventral body wall defects (VBWDs) were quite noticeable. VBWDs are congenital malformations of anterior abdominal wall in which abdominal viscera protrude out of the ventral body wall. Herein, an attempt was made to understand the changes the Ci provoked in the early embryos which might have led to the VBWDs. For this, before incubation, the chick embryos were dosed with the test chemical and then at different developmental stages of incubation, they were monitored for the changes in the expression of certain genes, which are indispensable for the ventral body wall closure since they regulate the cell fate, proliferation and survival. Concurrently, histopathological changes during

the embryonic development were examined to corroborate the above observations. The results of mRNA profiling revealed a significant downregulation of SHH on day 4 and upregulation in day 10, while *BMP4, PITX2, CDH1, WNT11, WNT6, PXN, MYOD1, CASPASE 3, AHR, CYP3A4*, showed a significant upregulation on day 4 and/or on day 10. *CDH2, FGF8, BMP1* showed no significant changes. The possible means by which these skewed expression patterns of regulatory molecules culminated into the VBWD (Figure 3.16) are discussed.

Tables

Group	Day 2 (Stage-13)	
	Somite number	% of embryos with abnormal somites
Control	18 (17, 19)	6.0 ± 0.57
Treated	16 (15, 18) *	33 ± 1.73 **

Table 3.1: Reduction in somite numbers: Values are expressed as mode with range in parenthesis; n=3 with 30 eggs per group per experiment; *$p \leq 0.05$, **$p \leq 0.01$.

Group	Day 2	Day 4	Day 10
Control	3.66 ± 0.19	3 ± 0.28	3.66 ± 0.50
Treated	10.66 ± 0.35**	12.33 ± 0.57***	14.66 ± 0.58***

Table 3.2: Mortality on day 2, day 4 and day 10 for sub-lethal dose Combination insecticide: The values represent mean ± standard error of mean; n=3 with 30 eggs per group per experiment; **$p \leq 0.01$, ***$p \leq 0.001$.

Group	Number of live embryos of Day 10	% of embryos with malformations
Control	26.33 ± 0.52	7.6 ± 0.52
Treated	15.33 ± 0.58***	60.6 ± 1.18***

Table 3.3: Percent malformation on day 10 from live embryos: The values represent mean ± standard error of mean; n=3 with 30 eggs per group per experiment; ***$p \leq 0.001$.

Gene	Mean ± SEM
SHH	0.0048 ± 0.0005***
BMP4	549.87 ± 55.200***
PITX2	9.87 ± 0.970*
CDH1	513.2 ± 52.412***
CDH2	0.920188 ± 0.097
FGF8	1.25 ± 0.140
CASPASE-3	300.025 ± 28.920***

Table 3.4: Fold change in mRNA of genes regulating somitogenesis on day 4 in 0.05µg/egg dose group. Fold change values for control embryo is 1.0 for all the genes. *p<0.05 and ***p<0.001.

Gene	Mean ± SEM
SHH	158.89 ± 16.212***
CDH1	247.89 ± 25.900***
WNT11	156.89 ± 15.901***
WNT6	278.89 ± 29.701***
VIMENTIN	1.23 ± 0.097
PXN	8.7 ± 0.920*
BMP1	1.1 ± 0.111
MYOD1	54.87 ± 5.903**
PCNA	0.0012 ± 0.0001***
CASPASE-3	378.92 ± 38.060***
AHR	471.58± 48.899***
CYP1A1	0.32 ± 0.039*
CYP3A4	289.87 ± 29.911***
CYP3A5	0.078 ± 0.008**

Table 3.5: Fold change in mRNA of genes involved in closure of ventral body wall folds on day 10 in 0.05µg/egg dose group. Fold change values for control embryo is 1.0 for all the genes. *p<0.05, **p<0.01, ***p<0.001

Protein	Values in arbitrary units	
Day 4		
SHH	44.21 ± 1.24	30.38 ± 0.91***
B-ACTIN	91.58 ± 0.61	93.17 ± 0.63
Day 10		
E-CADHERIN	55.35 ± 2.15	71.28 ± 0.85**
CL. CASPASE3	20.74 ± 1.35	88.41 ± 0.94***
B-ACTIN	95.35 ± 0.73	94.25 ± 0.38

Table 3.6: Spot densitometry analysis of the western blot bands on day 4 and 10 from live embryos. The Values represent Mean ± standard error of mean; n=3 with 10 eggs per group per experiment; **p≤0.01, ***p≤0.001

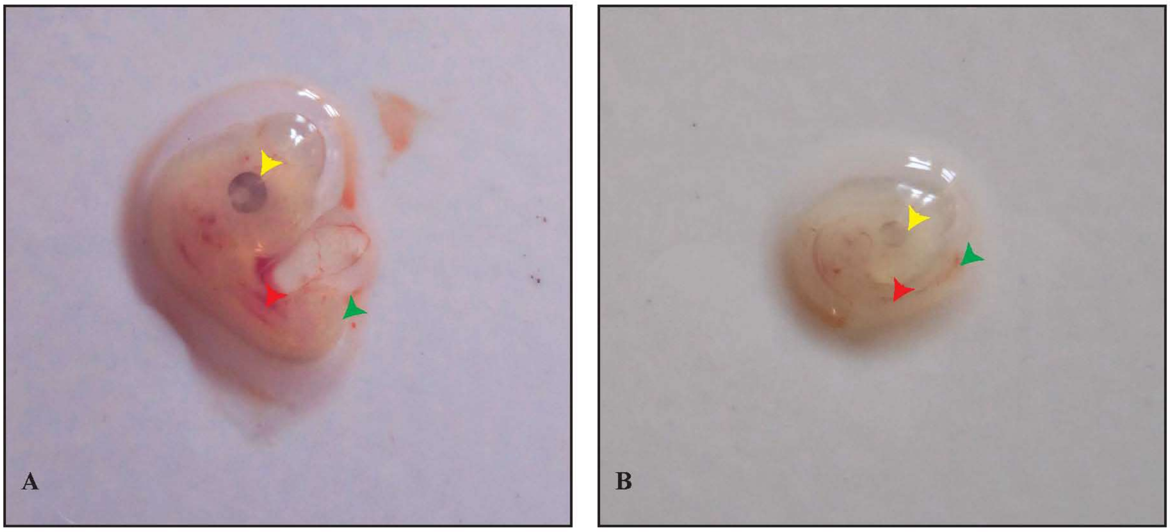

Figure 3.5: Ci induced structural anomalies: A) Control embryo of day 4 with well-developed eye (yellow arrowhead) and limb buds (red arrowhead); B) Ci treated day 4 embryo with under-developed eye (yellow arrowhead) and appendages (red arrowhead). Green arrow indicates the tail of the embryo.

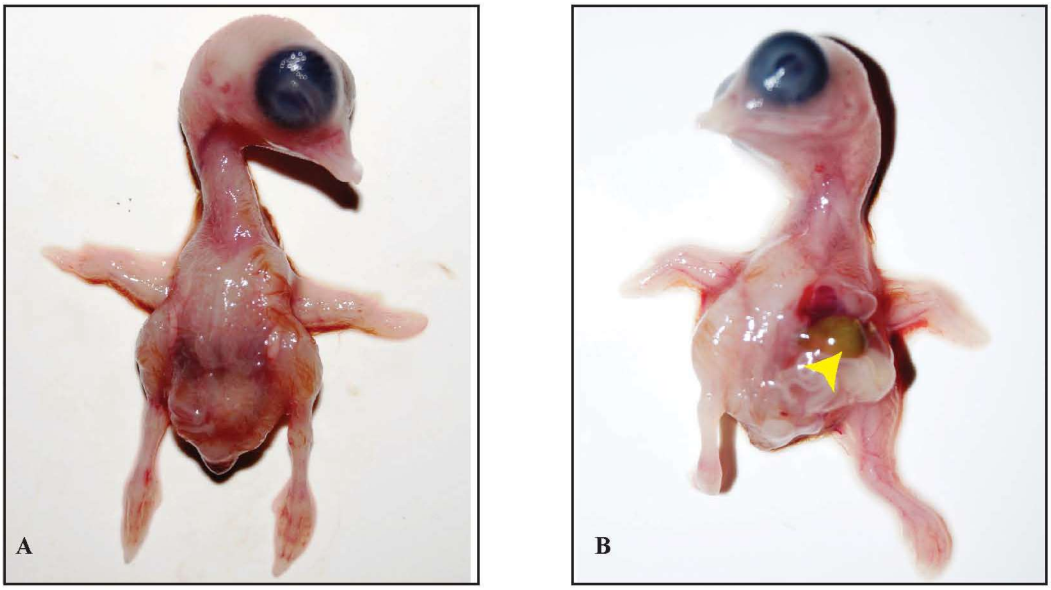

Figure 3.6: Ci induced structural malformations: A) Control embryo of day10; B) Ci treated day 10 embryo indicating protrusion of heart, liver and bowel without any covering sac in the treated embryo (Yellow arrowhead).

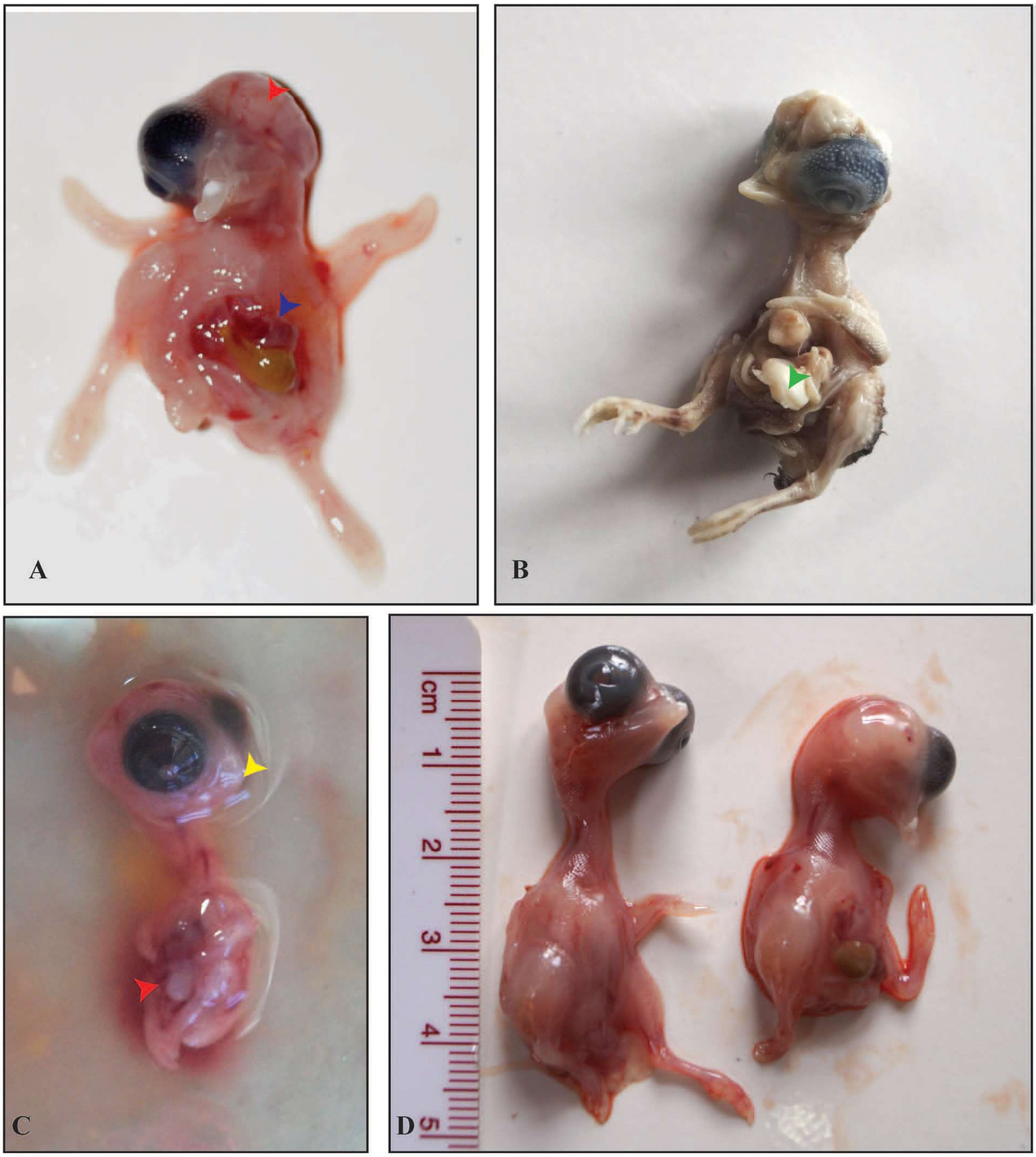

Figure 3.7: Ci treated day 10 embryos showing ventral body wall closure defects and associated anomalies: A) Protrusion of internal organs (Blue arrow) and anophthalmia (Red arrow); B) Formalin fixed treated embryo showing defect (herniation of visceral organs) (Green arrow) ; C) Absence of beak (Yellow arrow) and underdeveloped organs (Red arrow); D) Treated embryo with anophthalmia and reduction in size as compared to control embryo

Figure 3.8: Photomicrograph of day 4 chick embryo: longitudinal sections of A) Control embryo with well patterned structures; B) Treated embryo with reduced somites and distorted optic cup. Where, a: Myelencephalon, b: Somite, c: ventricle, d: Atrium, e: Liver-prominence, f: optic cup.

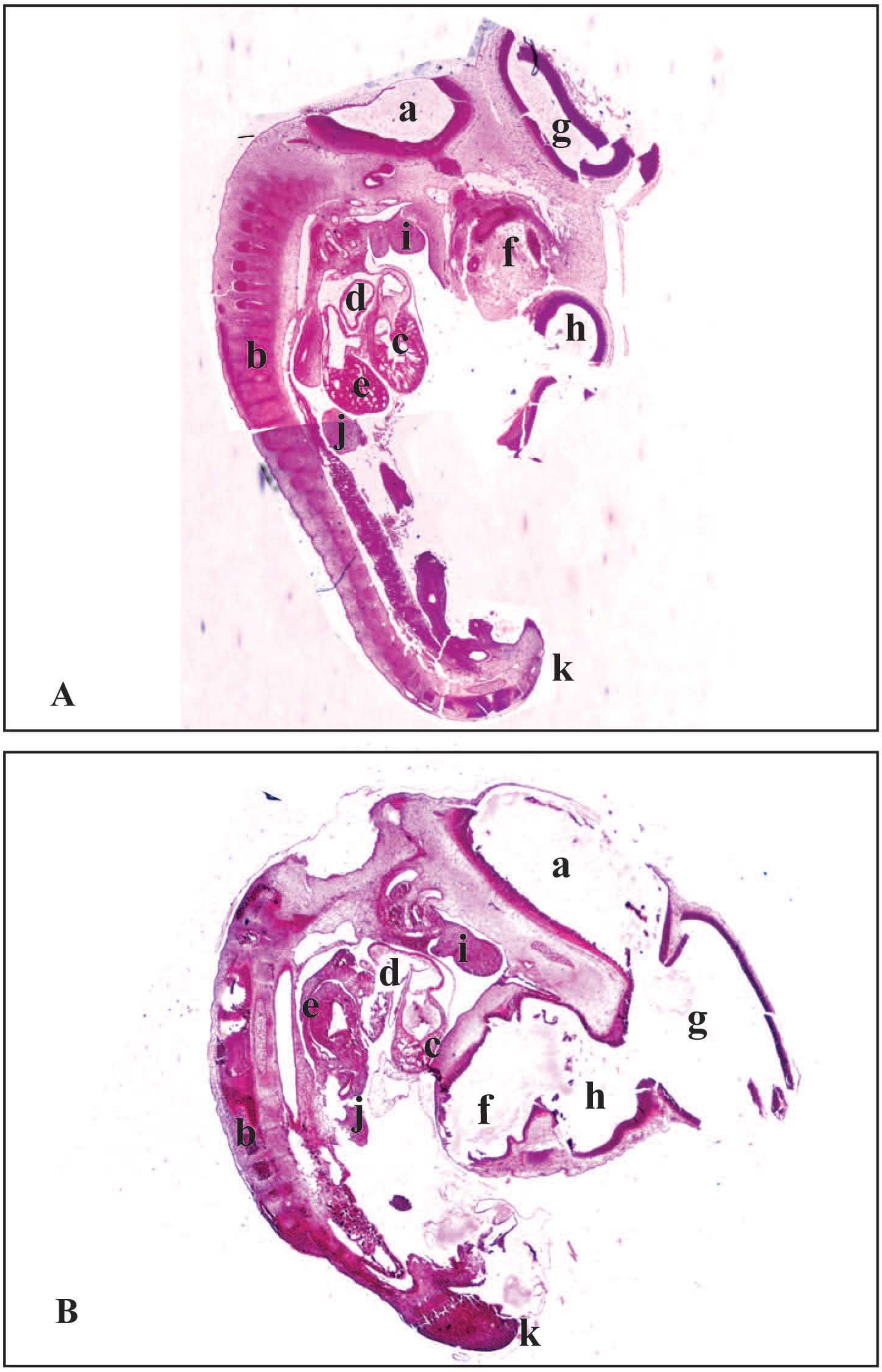

Figure 3.9: Composite images of day 4 chick embryo: longitudinal sections of A) Control embryo; B) Treated embryo. Where, a: Myelencephalon, b: Somite, c: ventricle, d: Atrium, e: Liver-prominence, f: optic cup, g: Mesencephalon, h: diencephalon, i: Visceral arch, j: anterior appendage bud, k: tail.

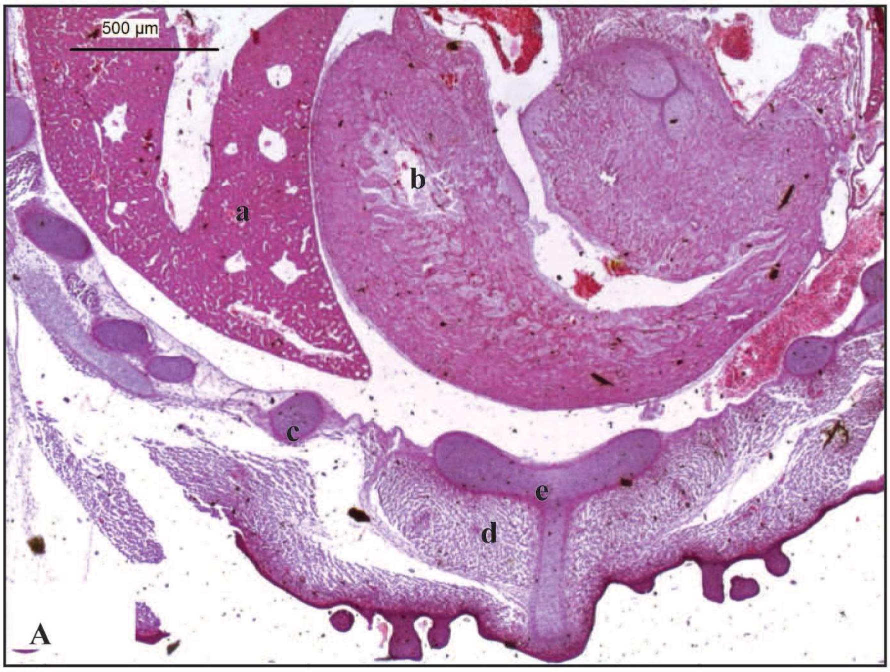

Figure 3.10: Cross section (insight) of abdominal region A) day 10 control embryo shows well-formed abdominal wall; B) day 10 Treated embryo showing improper closure of the ventral part of the body. Where, a: liver, b: stomach, c: Inter coastal muscles, d: Cartilage, e: Sternum.

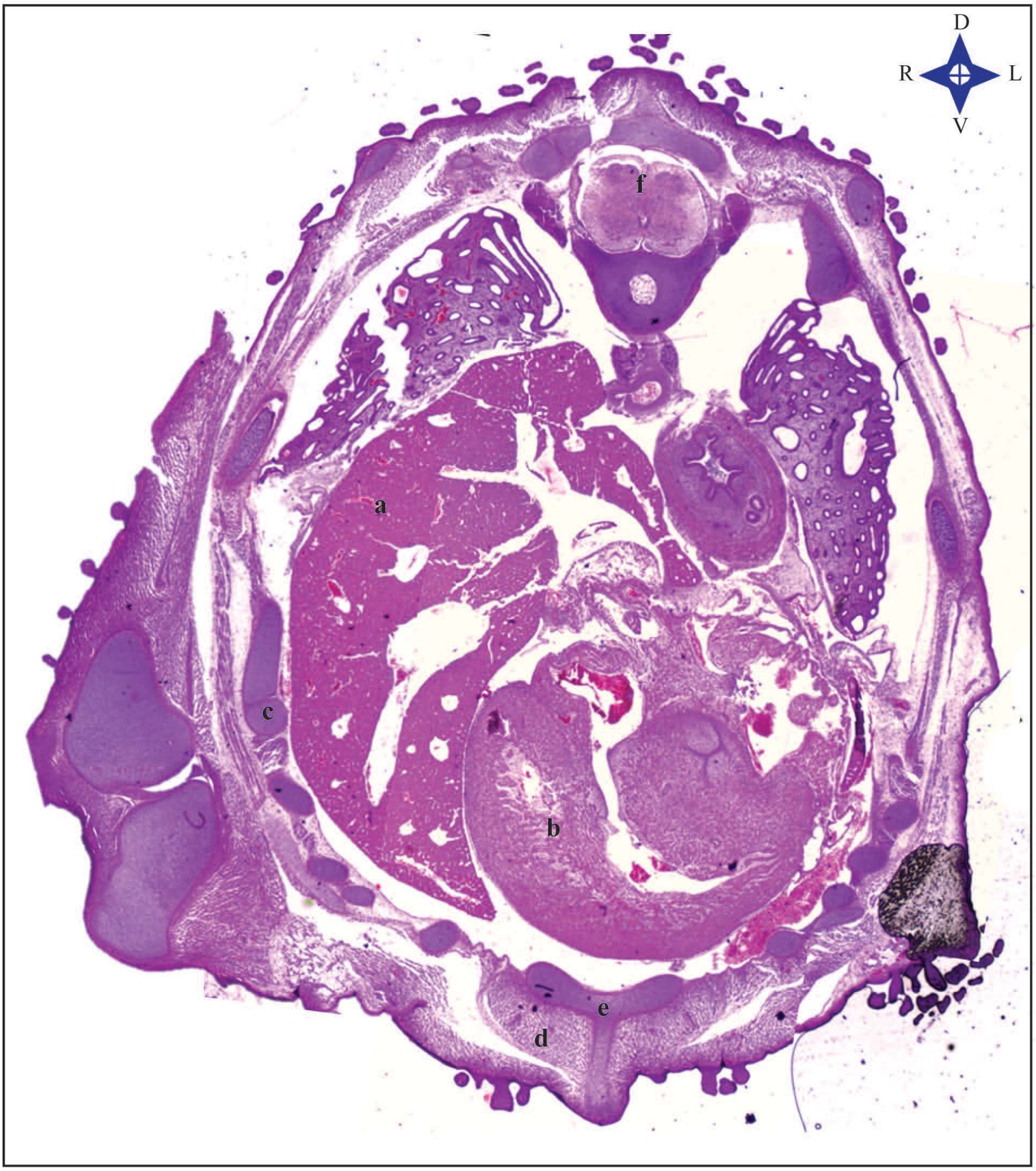

Figure 3.11: Composite image of cross section of day 10 chick embryo showing well-formed abdominal wall. Where, a: liver, b: stomach, c: Inter coastal muscles, d: Cartilage, e: sternum, f: vertebral column. The axis shows D: Dorsal, V: Ventral, R: Right and L: Left.

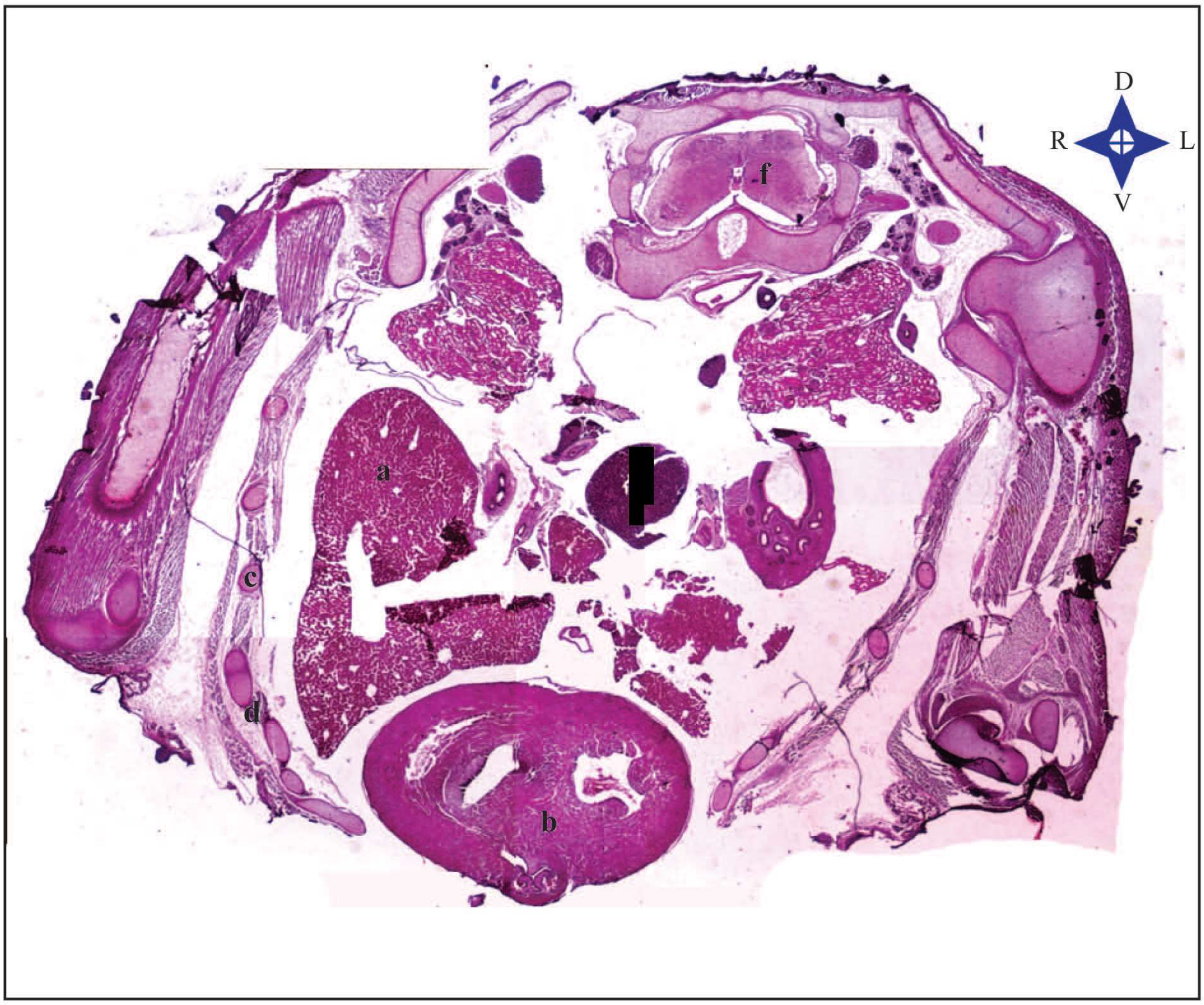

Figure 3.12: Composite image of cross section of day 10 chick embryo treated with combination insecticide showing distorted tissue architecture along with absence of sternum and ventral body wall. Where, a: liver, b: stomach, c: Inter coastal muscles, d: Cartilage, e: sternum (absent in treated group), f: vertebral column. The axis shows D: Dorsal, V: Ventral, R: Right and L: Left.

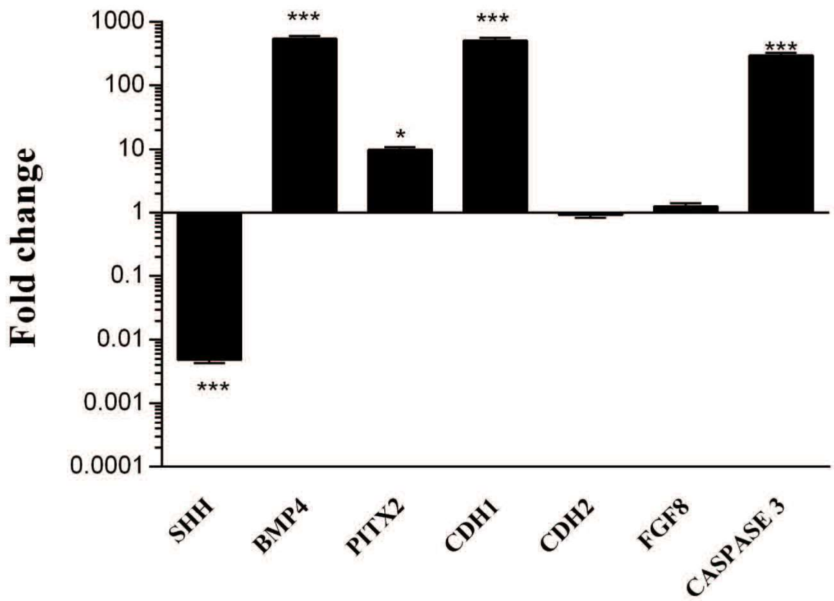

Figure 3.13: Transcript levels for Ci treated day 4 embryo: Fold change expression values for the genes. Fold change values for control embryo is 1.0 for all the genes, n=10 eggs/group. *: p ≤0.05; ***: p≤0.001

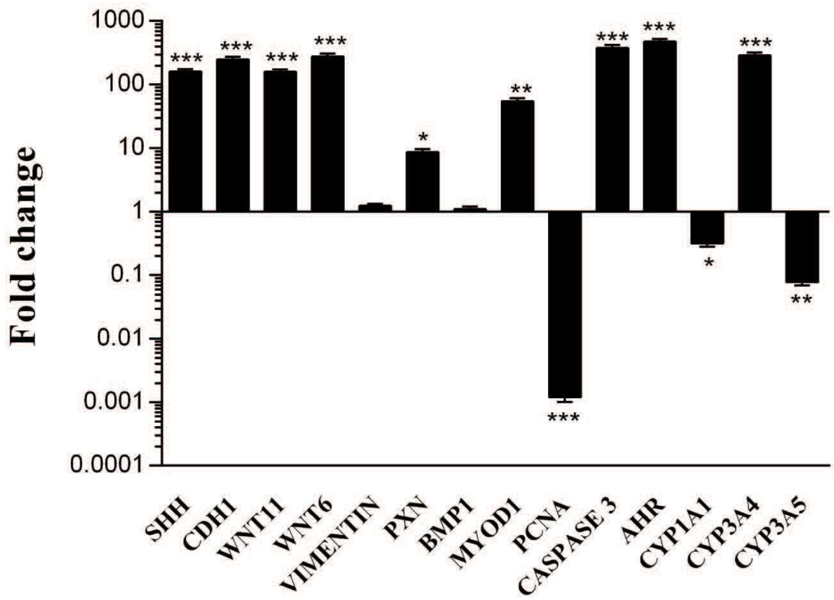

Figure 3.14: Figure 4: Transcript levels for Ci treated day 10 embryo: Fold change expression values for the genes. Fold change values for control embryo is 1.0 for all the genes, n=10 eggs/group. *: p≤0.05; **: p≤0.01; ***: p≤0.001

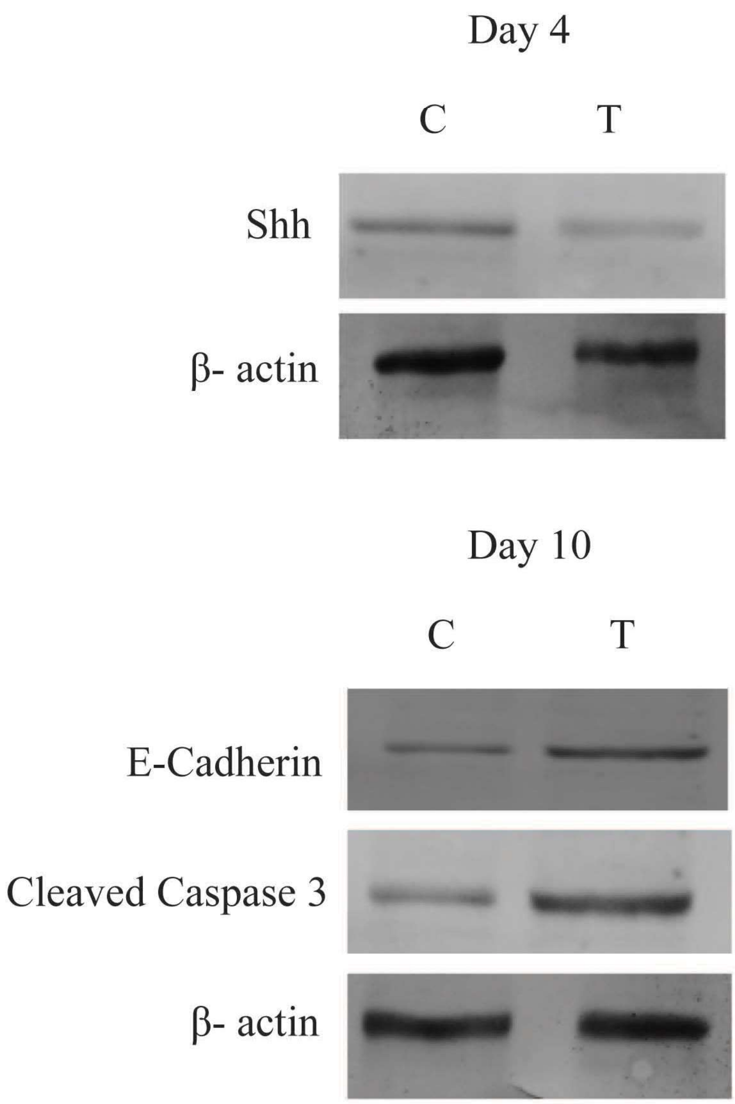

Figure 3.15: Western Blot images showing comparative expression of various proteins: Shh on day 4; E-Cadherin and Cleaved caspase-3 on day 10. β-actin was taken as loading control, n=10 eggs/group.

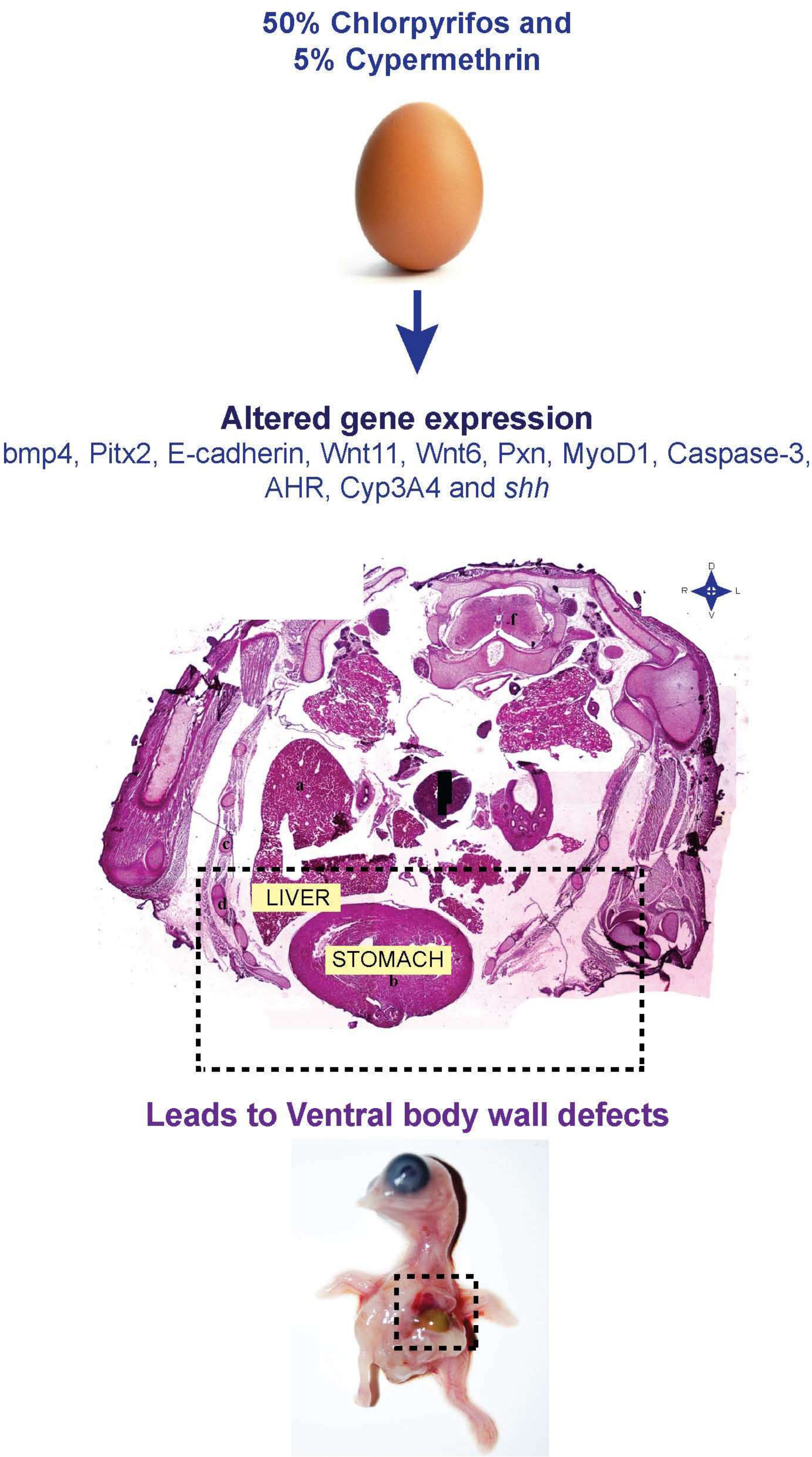

Figure 3.16: Graphical summary depicting effect of Ci on ventral body wall closure ascribed to altered gene expression